Available online at www.sciencedirect.com
ScienceDirect
Solid-State Electronics 51 (2007) 466–474
SOLID-STATE ELECTRONICS
www.elsevier.com/locate/sse

Transfer matrix method modelling of inhomogeneous Schottky barrier diodes on silicon carbide

M. Furno *, F. Bonani, G. Ghione

Dipartimento di Elettronica, Politecnico di Torino, Corso Duca Degli Abruzzi 24, 10129 Torino, Italy

Received 26 July 2006; received in revised form 3 January 2007; accepted 30 January 2007

The review of this paper was arranged by Prof. Y. Arakawa

Abstract

The paper presents a novel modelling technique for the static characteristics of power Schottky barrier diodes on SiC. Starting from an accurate and physically sound estimation of the transmission coefficient for the electrons movement across the Schottky barrier, the forward and reverse bias static current is evaluated and compared to experimental results. In order to properly reproduce experimental results, an inhomogeneous parallel conduction description of the Schottky barrier is shown to be required in reverse bias. Furthermore, consistently with previous work, a Schottky barrier height reduction is observed in moving from forward to reverse bias.

PACS: 73.30.+y; 73.40.Gk; 85.30.De

Keywords: 4H-SiC; Schottky barrier diode; Tunnelling; Transfer matrix method; Parallel conduction model

1. Introduction

The silicon carbide semiconductor device technology has reached during the last few years a satisfactory level of maturity. In particular, Schottky junction based SiC devices have demonstrated appealing features due to the process simplicity when compared to conventional or MIS junction devices. Examples of such devices are both power Schottky diodes, with strategic applications in switch mode power supplies, power factor correction, motor drives, output rectification, and MESFET transistors for the RF and low microwave ranges. Power Schottky barrier diodes (SBD) are indeed an example of well-consolidated SiC-based device, already sparsely present on the electronic market. Their close-to-ideal performances permit to fully exploit the superior material properties, namely high breakdown field and high thermal conductivity. A few semiconductor manufacturers offer SiC SBDs for applications in the medium power range (300–1200 V, 1–20 A) where low or zero switching losses are required.

To fully exploit the potentiality of SiC-based Schottky barrier devices, accurate compact models are required for circuit design. Despite the fair technological maturity achieved by such devices, models for their electrical characteristics are still not completely satisfactory. Deviations of silicon carbide SBD characteristics from the predictions of the thermionic emission (TE) model make conventional compact models for Schottky rectifiers not adequate. In the attempt to achieve a better understanding of the SiC-based SBDs, models of increasing complexity have been proposed in the literature; although such models are of course unsuited for circuit simulations, a deeper insight into the dominant conduction mechanisms in SiC-based SBDs can be ultimately helpful in designing more accurate compact models.

Although the forward bias operation of SiC SBDs is essentially in agreement with the TE model for

* Corresponding author. Tel.: +39 011 564 4003; fax: +39 011 564 4099.
E-mail address: mauro.furno@polito.it (M. Furno).

0038-1101/$ - see front matter © 2007 Elsevier Ltd. All rights reserved.
doi:10.1016/j.sse.2007.01.028

homogeneous Schottky interfaces, the reverse leakage current of such devices is many orders of magnitude higher than the TE model predictions [1–4]; even the inclusion of the image force barrier lowering (IFBL) does not allow to achieve reasonable agreement with experimental data. The exponential dependence on the applied bias voltage of the reverse leakage current of SiC SBDs suggests that tunnelling processes occur at the silicon carbide – Schottky metal interface. The calculation of such a tunnelling current was firstly attempted by Crofton and Sriram [1] exploiting the WKB approximation. Refinements of the model were then proposed in [2] and [4]. In [2], the influence of SBH random fluctuations on the electrical characteristics of SiC SBDs was also discussed. Nevertheless, the models [1,2,4] fail to provide a comprehensive description of the electrical behaviour of state-of-the-art silicon carbide SBDs.

The aim of the present paper is to develop an improved model for the forward and reverse characteristics of silicon carbide power SBDs. In order to gain a better insight into the device physics, an improved rigorous model for the calculation of the tunnelling current through the Schottky interface was developed, and coupled with an inhomogeneous barrier model. The resulting model is a compromise between a low number of physical assumptions and a reasonable number of fitting parameters. Comparison of the calculated characteristics with previously reported models and measured data allows to extract some physically sound model characteristics that can serve as a basis for the development of simplified compact models.

The paper is structured as follows. Section 2 is devoted to the description of the modelling strategy adopted, both for the homogenous and inhomogeneous description of the SBH. The model derived is validated against experimental data, both in forward and reverse bias, in Section 3, while some conclusions are drawn in Section 4.

2. The Schottky barrier model

In the present section we will first address the modelling of a homogeneous Schottky barrier. The treatment of inhomogeneous barrier is discussed in Section 2.2.

2.1. Homogeneous barriers

The 1D potential barrier profile at the Schottky metal–semiconductor interface is shown in Fig. 1. The potential energy profile $U(x)$ as a function of the distance from the Schottky interface (located at $x = 0$) can be written as [2]:

$$U(x) = \frac{q^2 N_D}{2\epsilon_s}(D - x)^2 - \frac{q^2}{16\pi\epsilon_s x}, \tag{1}$$

where N_D is the semiconductor (n-type) doping concentration, ϵ_s the semiconductor permittivity. D is the depletion region width, dependent on the bias voltage V applied to the Schottky contact and on the SBH ϕ_B according to:

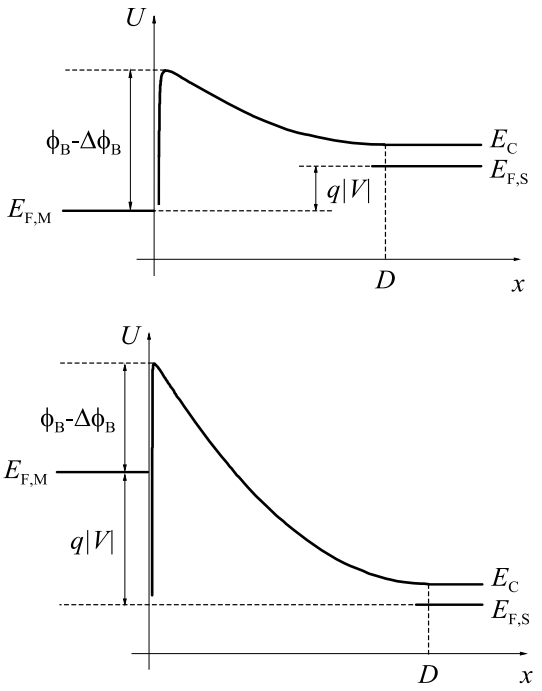

Fig. 1. Schematic representation of the band diagram at the Schottky interface incorporating the depletion and the IFBL contributions. Forward (above) and reverse (below) bias conditions.

$$D = \sqrt{\frac{2\epsilon_s}{qN_D}(V_{bi} - V)}, \tag{2}$$

$$qV_{bi} = \phi_B - (E_c - E_{F,S}). \tag{3}$$

The first term in (1) is the conventional parabolic depletion potential for a Schottky interface, which is referred to the bottom of the conduction band in the neutral semiconductor. The second term is the image force potential term, added to the depletion component as a first-order perturbation. The effect of the image force potential is a bias-dependent reduction $\Delta\phi_B$ in SBH. The SBH lowering $\Delta\phi_B$ calculated according to (1) well agrees with the conventional thermionic emission IFBL term (see, e.g., [5])

$$\Delta\phi_B = q\left[\frac{q^3 N_D(V_{bi} - V)}{8\pi^2\epsilon_s^3}\right]^{1/4}. \tag{4}$$

The net electron current density flowing from neutral semiconductor to metal through the Schottky potential barrier in Fig. 1 is calculated according to the Tsu–Esaki formalism [6,7]. In the general three-dimensional case, the electron current density J_{SM} from semiconductor to metal is proportional to the quantum transmitting coefficient $T(E_x)$ multiplied by the occupation probability in the metal $f_M(E)$ and the unoccupied probability in the semiconductor $1 - f_S(E)$. The metal–semiconductor current density J_{MS} is calculated in analogy. The net current density J is then given by the difference [8]:

$$J = J_{SM} - J_{MS} = \frac{qm^*}{2\pi^2\hbar^3}\int_{E_{min}}^{\infty} T(E_x)\cdot N(E_x)\mathrm{d}E_x, \tag{5}$$

$$N(E_x) = \int_0^{\infty} [f_M(E) - f_S(E)]\mathrm{d}E_{\parallel}. \quad (6)$$

The total kinetic energy E is decomposed as the sum of E_x, related to the velocity component v_x transversal to the Schottky barrier plane, and $E_{\parallel}$, associated to the velocity components parallel to the Schottky interface. The lower integration limit $E_{\min}$ in (5) is the minimum allowed energy value for the tunnelling process to occur. In our one-dimensional model, the transmission coefficient $T(E_x)$ is assumed to depend only on the transversal energy component E_x [7–9], and this allows to integrate (6) for the directions parallel to the Schottky barrier plane independently of the transmission coefficient. Moreover, under the assumption of isotropic cold Fermi–Dirac distributions of the electron populations in the metal and the semiconductor [8], the net current density J assumes the well-established form [1–3,6–9]:

$$J = \frac{qm^* k_B T}{2\pi^2\hbar^3} \int_{E_{\min}}^{\infty} T(E_x) \cdot \ln\left[\frac{1+\exp\left(\frac{E_{F,M}-E_x}{k_B T}\right)}{1+\exp\left(\frac{E_{F,S}-E_x}{k_B T}\right)}\right] \mathrm{d}E_x, \quad (7)$$

where $E_{F,M}$ and $E_{F,S}$ are the electron quasi-Fermi levels in the semiconductor and the metal, respectively. In the remainder of this article, the x dependence of the energy E is dropped for notational convenience. It is worth noticing that the current expression (7) self-consistently includes both the process of thermionic emission of carriers, i.e., emission for energy higher than the maximum of the potential Schottky barrier ($E > \phi_B - \Delta\phi_B$, Fig. 1), and tunnelling for the lower energy range ($E_{\min} < E < \phi_B - \Delta\phi_B$). Furthermore, the conventional formula for the thermionic emission current J_{TEIBL} with IFBL, which reads (see, e.g., [5]):

$$J_{TEIBL} = \frac{qm^* k_B^2 T^2}{2\pi^2\hbar^3} \exp\left[-\frac{q(\phi_B - \Delta\phi_B)}{k_B T}\right]\left[\exp\left(\frac{qV}{k_B T}\right) - 1\right], \quad (8)$$

is an approximation of (7). In fact, the thermionic emission current J_{TEIBL} is simply recovered from (7) by approximating the Fermi–Dirac statistics with the Maxwell–Boltzmann one, restricting the integration to energies higher than the maximum of the Schottky potential energy barrier (i.e., $E_{\min} = \phi_B - \Delta\phi_B$), and setting $T(E) = 1$. The full derivation of (8) from (7) is detailed in [10].

The calculation of the quantum-mechanical transmission coefficient $T(E)$ requires the solution of the one-dimensional Schrödinger equation for the potential (1). Since no closed-form solution exists, approximation or numerical techniques have to be employed. The most common approach is the Wentzel–Kramers–Brillouin (WKB) approximation [11], due to the ease of implementation and reduced computational cost. According to [11,12], the validity of such an approach is restricted to slowly varying potential profiles and to regions not too close to classical turning points. Moreover, the WKB approximation does not account for wavefunction reflections, which can have a crucial effect on the current density flowing through Schottky contacts. Therefore, numerical techniques [13–16] have to be preferred. Among numerical methods, the transfer matrix method (TMM) [17–19] is a powerful and relatively simple calculation approach, yielding very accurate results for a number of tunnelling problems (see, e.g., [4,8,9,17,20–23]).

According to TMM, an arbitrarily shaped potential barrier $U(x)$ is divided into layers. In each layer $U(x)$ is approximated by a constant or linear potential profile so that the Schrödinger equation admits of a closed-form solution. Due to the shape of the potential barrier under consideration (see Fig. 1), a piece-wise linear approximation scheme (with Airy functions expansion of the electron wavefunctions) is the most appropriate choice, allowing good accuracy to be achieved with a reduced number of layers [21,22,24]. This has clear advantages in terms of both the computational cost and the propagation of numerical errors. Thus, the Schottky potential barrier with width D is subdivided into N layers where the potential profile is assumed linear. The interface points between the subdivisions are labelled a_i, $i = 0,\ldots,N$. In the effective mass approximation, the time-independent Schrödinger equation associated to the motion of the particle perpendicular to the barrier in the layer (a_i, a_{i+1}) admits of the following analytic solution:

$$\psi_i(x) = C_i \mathrm{Ai}(z_i) + D_i \mathrm{Bi}(z_i), \quad (9)$$

where $\psi_i(x)$ denotes the particle wavefunction, $\mathrm{Ai}(z_i)$ and $\mathrm{Bi}(z_i)$ are Airy functions [25], and C_i and D_i are coefficients to be determined by imposing the continuity conditions of the wavefunctions $\psi_i(x)$, together with their first derivatives $\psi_i'(x)$, at the N interfaces.[1] On applying the continuity conditions, a global (two-by-two) transfer matrix $\mathbf{M}$ is obtained as detailed in [10,19]. We are now able to write the formal result for the transmission probability $T(E)$ for motion of electrons across the Schottky potential barrier, which reads [10]:

$$T(E) = \frac{k_S}{k_M} \cdot \frac{4k_M^2}{(m_{21} - m_{12}k_M k_S)^2 + (k_S m_{22} + k_M m_{11})^2}, \quad (10)$$

where m_{ij} are the elements of the two by two transfer matrix $\mathbf{M}$, and k_M (k_S) the electron wavevector in the metal (neutral semiconductor) defined as:

$$k_M = \sqrt{2m^*(E - E_{F,M})/\hbar^2} \quad (11)$$

$$k_S = \sqrt{2m^*(E - E_c)/\hbar^2}. \quad (12)$$

Care must be applied in the implementation of the TMM solution to avoid numerical instabilities which are often

[1] A rigorous treatment of the problem of tunnelling at heterointerfaces would require the continuity of the derivative of the wavefunction divided by the electron effective mass m^* [22]. As no information about the fine atomic structure of the interfacial layers adjacent to the SiC–metal junction was at our disposal, we assumed a material-independent constant effective mass, estimated by fitting experimental data.

noticed in the case of thick potential energy barriers. In particular, the Airy functions are known to give numerical overflow for a positive large argument (i.e., when the potential slope is low); this was solved through implementation of the asymptotic expressions of the Airy functions [25] according to the approach proposed in [24]. Furthermore, the stability of the proposed calculation approach was carefully investigated by varying the parameters of the Schottky potential energy barrier (1), namely the SBH ϕ_B and the doping concentration N_D. The solutions obtained from our calculation algorithm did not exhibit numerical problems for a wide range of parameters.

2.2. Inhomogeneous barriers

In the case of inhomogeneous Schottky interfaces, the effect of random SBH variations on the barrier surface must be accounted for. In this work, the parallel conduction model was adopted [26,27]. Accordingly, the effect of surface inhomogeneities is modelled making use of a statistical distribution of barrier height values. The distribution function $P(\phi_B, \sigma)$ is assumed here half-gaussian with maximum value ϕ_{B0} and variance σ:

$$P(\phi_B, \sigma) = \frac{2}{\sqrt{2\pi\sigma^2}} \exp\left[-\frac{(\phi_B - \phi_{B0})^2}{2\sigma^2}\right], \quad \phi_B \leqslant \phi_{B0}. \tag{13}$$

The total current density $J(V, \sigma)$ under an external bias V applied to the Schottky contact is then given by:

$$J(V, \sigma) = \int_{\phi_{B,min}}^{\phi_{B0}} J_0(\phi_B, V) P(\phi_B, \sigma) d\phi_B, \tag{14}$$

where $J_0(\phi_B, V)$ is the current density under an applied bias V calculated from (7) for a barrier height value ϕ_B. The lower integration limit $\phi_{B,min}$ was set equal to $\phi_{B0} - 7\sigma$ in our implementation, due to the rapid decay of the statistical distribution function. The maximum SBH ϕ_{B0}, as well as the variance σ, are suggested in the literature to be in principle dependent on the applied bias V [26,27]. We neglected in our work such a dependence of the inhomogeneity parameters on the applied bias; however, as discussed in Section 3, we indeed find that different values for ϕ_{B0} allow for the best fit to be achieved with experimental data in forward and reverse bias.

Under forward bias, the effect of the unit area series resistance R_S must also be included. We assumed a constant R_S value for every non-interacting diode of the parallel conduction model. The resistive region of the I–V characteristic of the SBD under examination was linearly interpolated, obtaining for the device a specific series resistance $R_S = 7 \times 10^{-3}\ \Omega\,cm^2$.

3. Results

In this section, the model is validated against measurements on silicon carbide SBDs. The device under examination in this work is a Ti/4H-SiC Schottky barrier diode with junction termination extension assembled in a standard commercial package (TO220). The structure of the devices consists of a 7 μm n-type epitaxial layer (doping concentration around $10^{16}\ cm^{-3}$, determined by $C(V)$ characterization) grown on an n^+, 380 μm substrate with doping concentration $10^{18}\ cm^{-3}$. The back-side cathode ohmic contact is composed by a triple metallic layer (titanium, nickel, and silver). Electrical characterization was performed with conventional SMU237 and SMU238 Keithley Source Measure Units. The details concerning fabrication, optimization, and electrical characterization of the device are reported elsewhere [28,29]. The device was chosen as its $J(V)$ characteristics were well-representative of those measured on a large number of devices with close-to-ideal electrical behaviour.

The model described in the previous section was implemented in MATLAB. The model parameters to be adjusted to fit experimental data are here summarized:

- electron effective mass m^*;
- maximum Schottky barrier height ϕ_{B0};
- variance parameter of the half-gaussian barrier height distribution σ.

In Sections 3.1 and 3.2 the forward and reverse bias modelling are discussed, respectively. While in the forward bias operation consideration of barrier inhomogeneities is not mandatory to achieve a good fit with measured data, neglecting those under reverse bias leads to results orders of magnitude away from the experiment.

3.1. Forward bias modelling

The exponential region of the forward $J(V)$ characteristic of a homogeneous SBD is generally well approximated by the thermionic emission component J_{TEIBL} (see (8)) of the total current density J, and it may be also demonstrated that the effect of IFBL are negligible under forward bias. It is apparent that if (8) holds, variations of the effective mass value m^* may be compensated by very small adjustments of the SBH. Let us assume for the moment $m^* = 0.3\,m_0$; this choice will be motivated later on.

The forward characteristic of the Ti/4H-SiC SBD is plotted in Fig. 2 and compared with the results of the thermionic emission model assuming a homogeneous barrier. In the same figure, the results of the complete quantum mechanical description in (7), employing both the WKB approximation and the TMM approach, are also shown. A barrier height value $\phi_{B0} = 1.21$ eV was extracted from the characteristic. The analysis of the calculated data shows that the WKB approximation gives higher current values with respect to the thermionic emission model: this because the thermionic emission model can be derived from the WKB description neglecting the contribution of tunnelling electrons. The TMM approach, instead, predicts lower currents due to the effect of wavefunction reflections, which

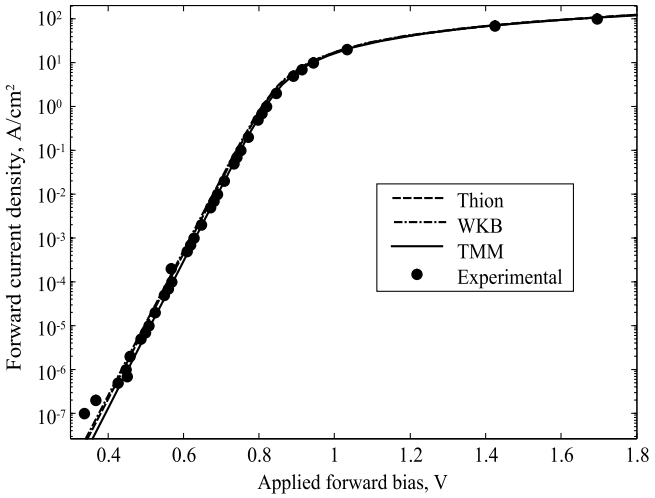

Fig. 2. Calculation results (lines) for a homogeneous SiC SBD under forward bias, $m^* = 0.3m_0$, $\phi_{B0} = 1.21$ eV, and comparison with experimental data (symbols).

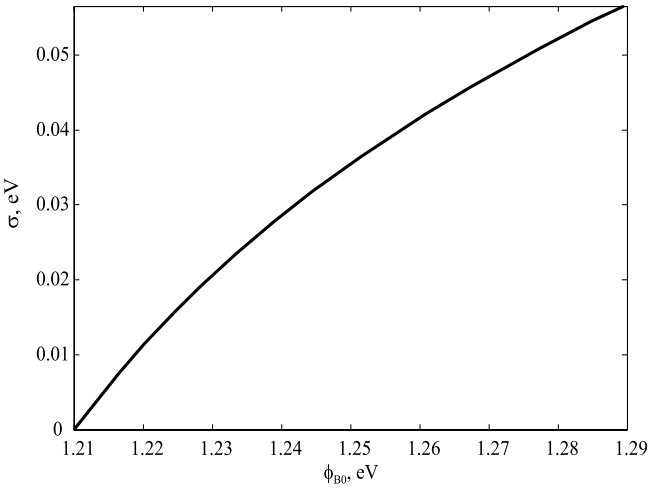

Fig. 3. Best (ϕ_{B0}, σ) values for the fit of the exponential region of the forward characteristic.

are neglected by the WKB approximation and in the thermionic emission model. The difference between the predictions of the different models lies in the range 50%–100%. We can conclude that a rigorous description of the forward characteristics of SBDs should include all quantum mechanical effects. However, a slight increase of the barrier height value may be employed in practice to compensate the neglected quantum mechanical effects.

Let us relax now the assumption of barrier homogeneity; we have to determine the values (ϕ_{B0}, σ) allowing for the best fit to experimental data by means of a numerical procedure; in fact, the variance σ of the barrier height distribution cannot be directly extracted from experiments. A lookup table was generated starting from the TMM implementation of (7) for various values of the SBH; the effect of the specific series resistance R_S was then included and the current contributions averaged according to (14). The locus in the plane (ϕ_{B0}, σ) shown in Fig. 3 was obtained by applying the least-square method between experimental and calculated data in the exponential region of the forward characteristic. When $\sigma \to 0$, a barrier height value $\phi_{B0} = 1.21$ eV is obtained, in close agreement with the value determined employing the homogeneous barrier model. When the variance is increased, the required barrier height correspondingly increases, as expected from theory (see (14)). The extracted values are collected in Table 1.

Table 1
Barrier height values extracted from the forward ($\phi_{B0,fwd}$) and reverse ($\phi_{B0,rev}$) characteristics as a function of σ

σ (eV)	$\phi_{B0,fwd}$ (eV)	$\phi_{B0,rev}$ (eV)
0.00	1.210	1.012
0.01	1.218	1.021
0.02	1.229	1.032
0.03	1.242	1.044
0.04	1.258	1.059
0.05	1.276	1.077

Fig. 4 shows the region of the forward characteristic where the onset of the resistive voltage drop of $J(V)$ occurs. Experimental results are compared with the data calculated for the (ϕ_{B0}, σ) values in Table 1. Although the agreement is very good for any (ϕ_{B0}, σ) value if the effect of the series resistance is negligible (i.e., for $V < 0.75$ V, outside the range shown in Fig. 4), for higher current values the bending of the calculated characteristic occurs for different bias values as a function of the variance of the SBH distribution σ, see Fig. 4. This because the resistive voltage drop of low SBH

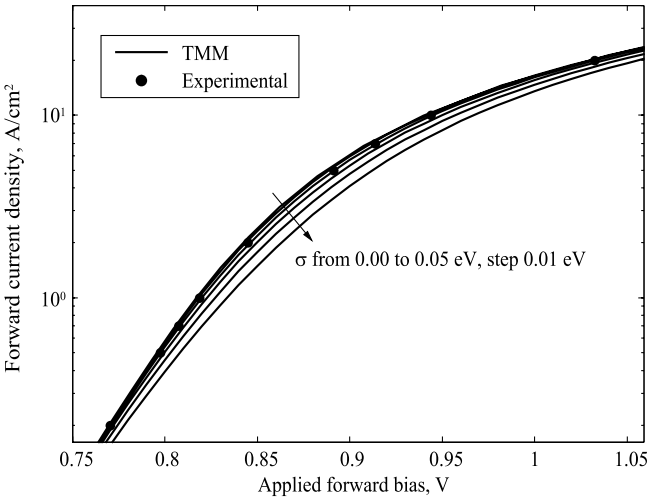

Fig. 4. Onset of the resistive bending of the device forward characteristic. Measured data (symbols) and calculation results for various (ϕ_{B0}, σ) values (lines).

regions is higher, and therefore their characteristic bends for lower applied bias voltages. The best fit is achieved for $\sigma = 0.02$ eV; such a rather low variance value (see, [2], for example) suggests that the quality of the Schottky contact realized on the SBD is very good. Similar results, which are not reported here, were obtained employing either the

thermionic emission model, or the WKB approximation. It can be concluded that the inclusion of barrier height inhomogeneities in the model for the SBD forward operation is not strictly necessary (apart from the second order effect of the resistive bending of the characteristic) if the quality of the Schottky contact under examination is very good. We will see in the next section that, on the other hand, the inclusion of SBH inhomogeneities is of crucial importance when dealing with the device reverse operation, even in the case of high quality Schottky interfaces.

3.2. Reverse bias modelling

In this section the modelling of the reverse bias operation of Ti/4H-SiC SBD is discussed. Let us begin as in the previous section by assuming a homogeneous Schottky interface, and then relax the homogeneity assumption.

The tunnelling transmission probability was calculated according to the WKB approximation and the TMM approach under an applied reverse bias of 500 V. The results are shown in Fig. 5. The tunnelling probability is underestimated by the WKB approach for energies a few eV lower than the potential energy maximum U_{max}. For higher energies, the exact tunnelling probability remains well below unity in a wide energy range, where the WKB approximation predicts a tunnelling probability close to 1. The reverse current densities calculated accordingly are shown in Fig. 6, and compared with the results achieved making use of the thermionic emission model with IFBL (TEIFBL). The TEIFBL model predicts reverse current values which are several orders of magnitude lower than those calculated employing the full quantum mechanical description in (7), as already discussed in the literature,

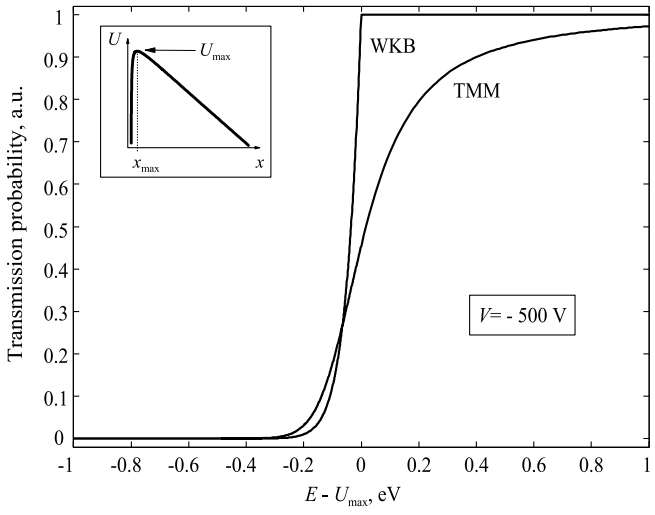

Fig. 5. Tunnelling transmission coefficient $T(E)$ as a function of the incident carrier energy relative to the potential energy maximum $E - U_{max}$. Comparison between the TMM and WKB approaches for an applied reverse bias of 500 V. The shape of the potential barrier in proximity of the Schottky interface is shown in the inset ($U_{max} = 500.76$ eV, $x_{max} = 0.55$ nm, and $dU/dx \simeq -0.11$ eV/nm for $x > x_{max}$).

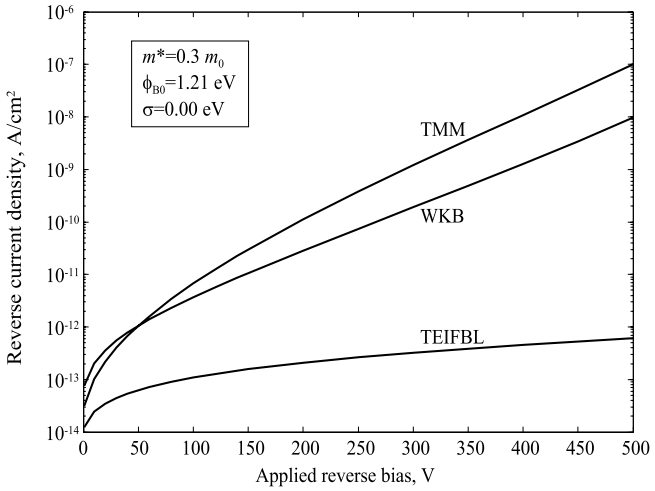

Fig. 6. Reverse current density calculated for a homogeneous SiC SBD according to various models (see text). The following parameter values were employed: $m^* = 0.3 m_0$, $\phi_{B0} = 1.21$ eV.

e.g., in [1,2,4,28]. On the other hand, both tunnelling models under examination, namely the WKB and the TMM approaches, predict higher currents. The main difference between the two approaches is the dependence of the calculated current on the applied bias voltage:

- the current calculated with the WKB approximation is higher for low reverse bias voltage (up to 50 V), where the thermionic emission current is still comparable to the tunnelling current;
- for higher voltages carrier tunnelling dominates and the current calculated with the TMM approach is higher. This because the WKB approximation underestimates the tunnelling transmission probability $T(E)$ for energies lower than the potential energy maximum, and the difference between the two approaches increases with increasing bias. For an applied reverse bias $V = 500$ V, the reverse current density calculated according to the WKB approximation is around one order of magnitude lower than the value achieved with the TMM approach, almost irrespectively of the SBH value.

As the quantitative predictions of the two tunnelling models differ of around one order of magnitude for a reverse bias voltage of 500 V, we shall restrict any further discussion to the results achieved with the TMM approach, due to its improved accuracy.

The electron effective mass m^* is the parameter determining the slope of the calculated reverse characteristics as shown in Fig. 7. The parameters employed in the calculation were those adjusted on the forward characteristic in the framework of the homogenous SBH model, i.e., $\sigma = 0$ eV and $\phi_{B0} = 1.21$ eV (see Table 1). One can notice that (i) the slopes of the experimental and calculated characteristics are in agreement for an effective mass value around $0.3 m_0$ and (ii) the modelled current is several orders of

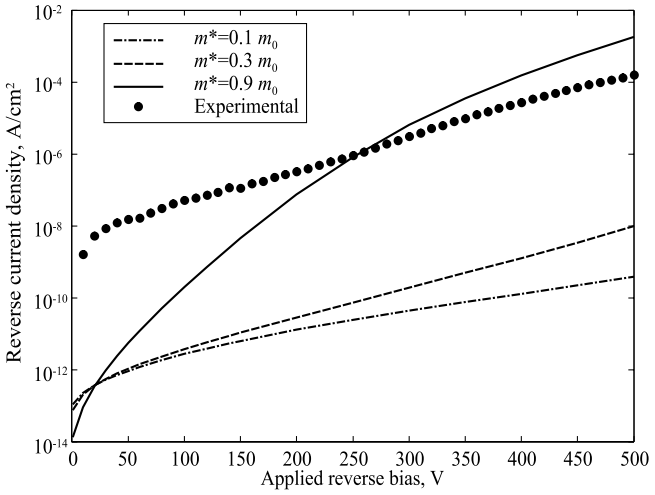

Fig. 7. Reverse current density calculated for a homogeneous SiC SBD according to the TMM approach for various m^* values ($\phi_{B0} = 1.21$ eV).

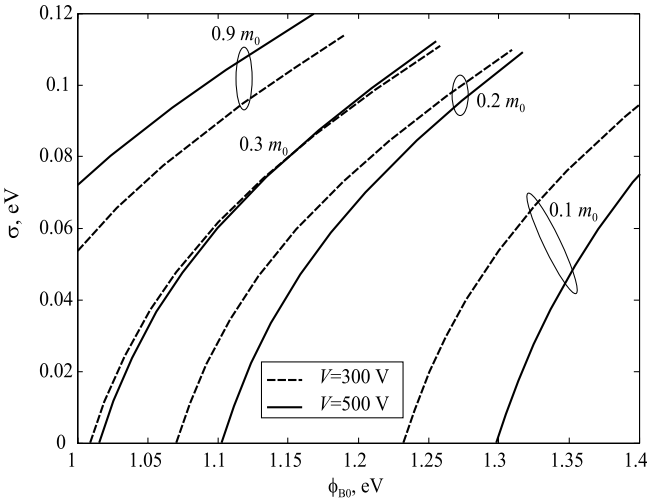

Fig. 8. Best (ϕ_{B0}, σ) values for the fit of the reverse characteristic. Calculations performed for two different bias points and for various effective mass values.

magnitude lower than the measurement when employing in the calculations an effective mass value well below m_0. As far as the effective mass is concerned, one may argue that a value $m^* = 0.3\,m_0$ is not consistent with theoretically calculated values. However, the discrepancy between theory and experiments is reported in a number of literature works (see, [4,29], for example), and it is usually ascribed to the defective nature of the Schottky interface. An experimental evaluation of m^* was performed in [29] in the framework of the thermionic emission model for the same device we are investigating, leading to $m^* \simeq 0.2\,m_0$, in fair agreement with the value extracted in this work. Once the effective mass value is determined from the slope of the experimental data, the SBH is the only remaining degree of freedom at our disposal to fit measurements, if a homogeneous Schottky interface is assumed. Satisfactory agreement with experiments was achieved employing a SBH value as low as 1.012 eV (not shown here). Such a value is much lower than the SBH value extracted from the forward characteristic (see, Table 1).

Relaxing the assumption of barrier homogeneity, the standard deviation σ of the SBH distribution in (13) is a further degree of freedom to fit the experimental $J(V)$ curves. A lookup table was generated for several values of ϕ_{B0} and σ, and the best values (ϕ_{B0}, σ) for the fit of the experimental data were determined through the least-square method. The calculations were performed for two different reverse bias points, 300 V and 500 V, and for several values of the electron effective mass m^*, with results shown in Fig. 8. An effective mass $m^* = 0.3\,m_0$ is the only value allowing to fit at the same time the measurements for the two bias points. This is consistent with the results in Fig. 7 and with the above remarks on the influence of the effective mass on the slope of the reverse characteristics, which can be extended to the inhomogeneous case. The maximum barrier height of the half-gaussian distribution ϕ_{B0} required to fit the measured data as a function of various σ values are collected in Table 1. Fig. 9 finally shows the calculated reverse characteristic employing a variance parameter $\sigma = 0.02$ eV, together with experimental data. The leakage current of the device under examination is well reproduced by our calculations over a wide bias range. The discrepancy in the lower reverse bias region can be traced back to edge-related effects which are not included in our 1D model [9,30]. In Fig. 9, the results achieved according to the WKB approach employing the same (ϕ_{B0}, σ) values are also given. Comparing Figs. 6 and 9, it can be noticed that the discrepancies between the two approaches remain the same taking into account or neglecting the effects of SBH inhomogeneities.

It may be finally noticed that the SBH values reported in Table 1 for the device reverse operation are lower than those obtained in the forward operation case by a (almost)

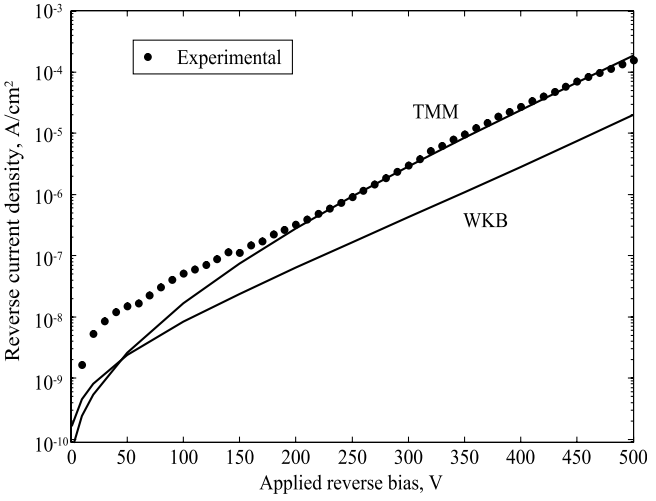

Fig. 9. Calculated reverse current density, $m^* = 0.3\,m_0$, $\phi_{B0} = 1.032$ eV, and $\sigma = 0.02$ eV. Results of the TMM and WKB approaches and comparison with experimental data.

constant value of 0.2 eV. Comparing Figs. 3 and 8, one may also observe that the curves do not show any intersection for any reasonable value of the parameters, coherently with the reduction in ϕ_{B0} in Table 1. This discrepancy could be, e.g., ascribed to interactions of low SBH regions with surrounding higher barrier regions [31,32]. Such interactions are neglected in the parallel conduction model employed in this work, where the contributions to the total current of low and high barrier regions are calculated independently.

4. Conclusion

We have presented in this paper a theoretical study on the electrical characteristics of SiC-based power SBDs. After evaluating state-of-the-art literature models, we have developed an improved model consisting of a rigorous description of electron tunnelling through the Schottky interface coupled with the parallel conduction model to account for SBH inhomogeneities. Our comprehensive model correctly predicts the characteristics of the device both under forward bias, where thermionic emission dominates, and under reverse bias, where the tunnelling current is the major contribution. A reduction in the barrier height value is noticed when moving from the forward to the reverse characteristic. Such a discrepancy in the SBH values is expected to be related to the interaction between low and high barrier regions, not accounted for in the parallel conduction model.

Acknowledgements

This work was initiated by a cooperation with International Rectifier Corporation Italiana S.p.A.: we thank L. Merlin and G. Richieri for helpful discussions. S. Ferrero and L. Scaltrito of Politecnico di Torino, Dipartimento di Fisica are gratefully acknowledged for providing the experimental results. Finally, the work has been partly supported by the Italian MIUR through the PRIN 2005 "FPFET" project.

References

[1] Crofton J, Sriram S. Reverse leakage current calculations for SiC Schottky contacts. IEEE Trans Electron Devices 1996;43(12):2305–7.
[2] Zheng L, Joshi RP, Fazi C. Effects of barrier height fluctuations and electron tunneling on the reverse characteristics of 6H-SiC Schottky contacts. J Appl Phys 1999;85(7):3701–7.
[3] Eriksson J, Rorsman N, Zirath H. 4H-silicon carbide Schottky barrier diodes for microwave applications Schottky. IEEE Trans Microwave Theory Technol 2003;51(3):796–804.
[4] Blasciuc-Dimitriu D, Horsfall AB, Wright NG, Johnson CM, Vassilevski KV, O'Neill AG. Quantum modelling of *I–V* characteristics for 4H-SiC Schottky barrier diodes. Semicond Sci Technol 2005;20(1):10–5.
[5] Rhoderick EH, Williams RH. Metal–semiconductor contacts. Oxford: Clarendon; 1988.
[6] Tsu R, Esaki L. Tunneling in a finite superlattice. Appl Phys Lett 1973;22(11):562–4.
[7] Fromhold Jr AT. Quantum mechanics for applied physics and engineering. New York: Academic Press; 1981.
[8] Gehring A, Selberherr S. Modeling of tunneling current and gate dielectric reliability for nonvolatile memory devices. IEEE Trans Device Mater Reliab 2004;4(3):306–19.
[9] Sassen S, Witzigmann B, Wölk C, Brugger H. Barrier height engineering on GaAs THz Schottky diodes by means of high–low doping, InGaAs- and InGaP-layers. IEEE Trans Electron Devices 2000;47(1):24–32.
[10] Furno M. PhD dissertation. Politecnico di Torino.
[11] Messiah A. Quantum Mechanics. Amsterdam: North-Holland; 1967.
[12] Ghatak AK, Sautery EG, Goyalz IC. Validity of the JWKB formula for a triangular potential barrier. Eur J Phys 1997;18:199–204.
[13] Lent CS, Kirkner DJ. The quantum transmitting boundary method. J Appl Phys 1990;67(10):6353–9.
[14] Nakamura K, Shimizu A, Koshiba M, Hayata K. Finite-element analysis of quantum wells of arbitrary semiconductors with arbitrary potential profiles. IEEE J Quantum Electron 1989;25(5):889–95.
[15] Roy S, Ghatak AK, Goyal IC, Gallawa RL. Modified Airy function method for the analysis of tunneling problems in optical waveguides and quantum-well structures. IEEE J Quantum Electron 1993;29(2):340–5.
[16] Zhang A, Cao Z, Shen Q, Dou X, Chen Y. Tunnelling coefficients across an arbitrary potential barrier. J Phys A 2000;33(30):5449–56.
[17] Ghatak AK, Thyagarajan K, Shenoy MR. Numerical analysis of planar optical waveguides using matrix approach. J Lightwave Technol 1987;LT-5(5):660–7.
[18] Ando Y, Itoh T. Calculation of transmission tunneling current across arbitrary potential barriers. J Appl Phys 1987;61(4):1497–502.
[19] Lui WW, Fukuma M. Exact solution of the Schrödinger equation across an arbitrary one-dimensional piecewise-linear potential barrier. J Appl Phys 1986;60(5):1555–9.
[20] Ghatak AK, Thyagarajan K, Shenoy MR. A novel numerical technique for solving the one-dimensional Schrödinger equation using matrix approach – Application to quantum well structures. IEEE J Quantum Electron 1988;24(8):1524–31.
[21] Allen SS, Richardson SL. Theoretical investigations of resonant tunneling in asymmetric multibarrier semiconductor heterostructures in an applied constant electric field. Phys Rev B 1994;50(6):11693–700.
[22] Jonsson B, Eng TE. Solving the Schrödinger equation in arbitrary quantum-well potential profiles using the transfer matrix method. IEEE J Quantum Electron 1990;26(11):2025–35.
[23] Vega AR. Comparison study of tunneling models for Schottky field effect transistors and the effect of Schottky barrier lowering. IEEE Trans Electron Devices 2006;53(7):1593–600.
[24] Vatannia S, Gildenblat G. Airy's function implementation of the transfer-matrix method for resonant tunneling in variably spaced finite superlattices. IEEE J Quantum Electron 1996;32(6):1093–105.
[25] Abramowitz M, Stegun IA. Handbook of mathematical functions. New York: Dover; 1964.
[26] Werner JH, Guttler HH. Barrier inhomogeneities at Schottky contacts. J Appl Phys 1991;69(3):1522–33.
[27] Chand S, Kumar J. Simulation and analysis of the *IV* characteristics of a Schottky diode containing barrier inhomogeneities. Semicond Sci Technol 1997;12:899–906.
[28] Furno M, Bonani F, Ghione G, Ferrero S, Porro S, Mandracci P, et al. Design, fabrication, and characterization of 1.5 $m\Omega\,cm^2$, 800 V 4H-SiC n-type Schottky barrier diodes. Mater Sci Forum 2005;483–485:941–4.
[29] Pirri CF, Ferrero S, Scaltrito L, Perrone L, Guastella S, Furno M, et al. Intrinsic 4H-SiC parameters study by temperature behaviour analysis of Schottky diodes. Microelectron Eng 2006;83(1):86–8.
[30] Schoen KJ, Woodall JM, Cooper Jr JA, Melloch MR. Design considerations and experimental analysis of high-voltage SiC

Schottky barrier rectifiers. IEEE Trans Electron Devices 1998;45(7): 1595–604.
[31] Tung RT. Electron transport at metal–semiconductor interfaces: General theory. Phys Rev B 1992;45(23):13509–23.
[32] Ru G-P, Van Meirhaeghe RL, Forment S, Jiang Y-L, Qu X-P, Zhu S, et al. Voltage dependence of effective barrier height reduction in inhomogeneous Schottky diodes. Solid-State Electron 2005;49(4): 606–11.